© 2019. Published by The Company of Biologists Ltd | Journal of Experimental Biology (2019) 222, jeb200840. doi:10.1242/jeb.200840

RESEARCH ARTICLE

Optimal length, calcium sensitivity and twitch characteristics of skeletal muscles from *mdm* mice with a deletion in N2A titin

Anthony L. Hessel*,[1,‡], Venus Joumaa[2], Sydney Eck[1], Walter Herzog[2] and Kiisa C. Nishikawa[1]

ABSTRACT

During isometric contractions, the optimal length of skeletal muscles increases with decreasing activation. The underlying mechanism for this phenomenon is thought to be linked to length dependence of Ca^{2+} sensitivity. Muscular dystrophy with myositis (*mdm*), a recessive titin mutation in mice, was used as a tool to study the role of titin in activation dependence of optimal length and length dependence of Ca^{2+} sensitivity. We measured the shift in optimal length between tetanic and twitch stimulation in *mdm* and wild-type muscles, and the length dependence of Ca^{2+} sensitivity at short and long sarcomere lengths in *mdm* and wild-type fiber bundles. The results indicate that the *mdm* mutation leads to a loss of activation dependence of optimal length without the expected change in length dependence of Ca^{2+} sensitivity, demonstrating that these properties are not linked, as previously suggested. Furthermore, *mdm* muscles produced maximum tetanic stress during sub-optimal filament overlap at lengths similar to twitch contractions in both genotypes, but the difference explains less than half of the observed reduction in active force of *mdm* muscles. *Mdm* muscles also exhibited increased electromechanical delay, contraction and relaxation times, and decreased rate of force development in twitch contractions. We conclude that the small deletion in titin associated with *mdm* in skeletal muscles alters force production, suggesting an important regulatory role for titin in active force production. The molecular mechanisms for titin's role in regulating muscle force production remain to be elucidated.

KEY WORDS: Activation-dependent properties, Isometric force production, Force transmission, Length-dependent properties, Submaximal force production, Muscular dystrophy with myositis, Connectin

INTRODUCTION

In contracting striated muscles, force is produced when cross-bridges form cyclically between thick and thin filaments of muscle sarcomeres (Huxley, 1957). During maximum isometric activation, the magnitude of force is proportional to the overlap between actin and myosin filaments on the descending limb of the force–length relationship (Gordon et al., 1966). Despite this congruence of the force–length relationship with the sliding filament hypothesis (Huxley and Hanson, 1954; Huxley and Niedergerke, 1954), it has been shown that the force–length relationship shifts to longer sarcomere lengths as activation decreases (Bahler et al., 1967; Brown et al., 1999; Holt and Azizi, 2016; Holt and Williams, 2018). This 'activation dependence of optimal length' is noteworthy because skeletal muscles are rarely, if ever, activated maximally *in vivo* (Holt and Azizi, 2016). In whole-muscle preparations, part, but not all, of the shift is caused by fiber shortening against compliant series elastic elements (Bahler et al., 1967; Holt and Williams, 2018), such as tendons or aponeuroses, during force development. Although fiber shortening results in force depression, force depression alone does not account for the shift in muscle optimal length (Holt and Williams, 2018).

Activation dependence of optimal length is widely viewed as resulting from length-dependent activation, a phenomenon in which, given constant submaximal [Ca^{2+}], more force is produced at longer sarcomere lengths than is predicted by filament overlap (Rack and Westbury, 1969; Rassier et al., 1999; Stephenson and Wendt, 1984). The length dependence of Ca^{2+} sensitivity is considered to be a key component of length-dependent activation; for a given submaximal level of [Ca^{2+}], a larger level of activation is induced at longer, compared with shorter, sarcomere lengths (de Tombe et al., 2010; MacIntosh, 2017). This increase in relative activation level is thought to counteract the reduction in force owing to decreased filament overlap at longer sarcomere lengths, and leads to a shift of the force–length relationship toward longer lengths in submaximal contractions (Rassier et al., 1999; Stephenson and Wendt, 1984). Although this hypothesis is theoretically plausible, no studies demonstrate a causal link between length dependence of Ca^{2+} sensitivity and activation dependence of optimal length.

Titin is the third most abundant protein by weight in striated muscle (Wang et al., 1979), with isoforms specific to cardiac (N2B/N2BA) and skeletal (N2A) muscles (Freiburg et al., 2000). In skeletal muscles, alternative splicing within exons that code for the elastic I-band region leads to variability in titin length and mechanical properties, including titin stiffness, among different muscles (Freiburg et al., 2000; Linke, 2017; Prado et al., 2005). Titin stiffness increases upon activation in skeletal muscle (Labeit et al., 2003; Leonard and Herzog, 2010; Monroy et al., 2017; Powers et al., 2014). A small amount of this increase in active titin stiffness is likely due to Ca^{2+} binding to titin (Labeit et al., 2003), whereas the majority is thought to arise from a mechanical change in titin's elastic I-band region (Joumaa et al., 2007, 2008; Leonard and Herzog, 2010), perhaps by an activation-dependent interaction between titin and actin that shortens titin's free length (Dutta et al., 2018; Leonard and Herzog, 2010; Nishikawa et al., 2012).

Although it is well documented that changes in titin-based force affect Ca^{2+} sensitivity at specific sarcomere lengths (Fukuda et al., 2011; Mateja et al., 2013; Ottenheijm et al., 2012), the mechanism is elusive. It has been argued that titin force regulates Ca^{2+} sensitivity by mechanisms associated with a decrease in actin–myosin lattice

[1]Center for Bioengineering Innovation and Department of Biological Sciences, Northern Arizona University, Flagstaff, AZ 86011, USA. [2]Human Performance Laboratory, Faculty of Kinesiology, University of Calgary, Calgary, AB, Canada, T2N 1N4.
*Present address: Human Movement Science, Faculty of Sport Science, Ruhr University Bochum, Bochum, NRW 44801, Germany.

‡Author for correspondence (anthony.hessel@rub.de)

A.L.H., 0000-0001-6767-6345; V.J., 0000-0001-7720-881X; K.C.N., 0000-0001-8252-0285

Received 30 January 2019; Accepted 13 May 2019

spacing, and/or length-dependent strain of the thick filaments, which theoretically increase the number of cross-bridges and cross-bridge force in active muscle (Fukuda et al., 2011; Fusi et al., 2016; Konhilas et al., 2002b). However, Ma et al. (2018) recently demonstrated that thick filament rearrangement is similar during active and passive stretch, suggesting that thick filament strain in contracting muscle is simply an effect of stretch and is not associated with increased cross-bridge force. Furthermore, it has been shown that length-dependent activation differs between fast and slow muscles and these differences are likely attributed to titin and contractile protein isoform variations among fast and slow muscles (Gulati et al., 1991; Konhilas et al., 2002b; McDonald et al., 1997).

It is currently unknown whether activation-dependence of titin stiffness contributes to length dependence of Ca^{2+} sensitivity. The muscular dystrophy with myositis (*mdm*) mutation in mice provides a unique opportunity to test this hypothesis. The *mdm* mutation leads to an estimated 83 amino acid deletion in the I-band region of titin (Garvey et al., 2002). *Mdm* muscles fail to show an increase in stiffness upon muscle activation (Monroy et al., 2017; Powers et al., 2016). If titin contributes to length dependence of Ca^{2+} sensitivity and activation-dependence of optimal length, then these properties are expected to be reduced or absent in muscles from *mdm* mice.

The goal of this study was to evaluate the length dependence of activation and activation dependence of optimal length in skeletal muscles from wild-type and *mdm* mice. We examined two muscles in both genotypes, the predominantly slow-twitch soleus and predominantly fast-twitch extensor digitorum longus (EDL) (Kushmerick et al., 1992). Soleus and EDL muscles express different titin isoforms, with a relatively larger passive stiffness in EDL compared with soleus (Nocella et al., 2012; Prado et al., 2005). We first measured activation dependence of optimal length and length dependence of Ca^{2+} sensitivity. We then assessed force production during and after a twitch by examining electromechanical delay (EMD, also called latent period), rate of force development, contraction time and half relaxation time. Finally, we measured optimal sarcomere length during tetanic and twitch contractions using transmission electron microscopy. If the *mdm* mutation affects length-dependent activation and/or activation dependence of optimal length, then these properties should be reduced or absent in *mdm* compared with wild-type muscles.

MATERIALS AND METHODS

Ethical approval

Animal experiments were approved by the Institutional Animal Care and Use Committee of Northern Arizona University, which is accredited by the Association for Assessment and Accreditation of Laboratory Animal Care, International.

Whole muscle

Heterozygous mice (*Mus musculus* Linnaeus 1758) of the strain B6C3Fe a/a-Ttn mdm/J were obtained from the Jackson Laboratory (Bar Harbor, ME, USA). A breeding colony was established to obtain male and female wild type and homozygous recessive (*mdm*) mice (age range 23–29 days old). All mice had food and water *ad libitum*. During surgical procedures, anesthesia was induced by placing mice in a bell jar with isoflurane anesthesia, and was maintained during surgery by administration of an intraperitoneal ketamine (70–100 mg kg^{-1})/xylazine (5–10 mg kg^{-1}) injection. After surgery, mice were euthanized with an overdose of ketamine/xylazine followed by cervical dislocation.

Muscles were prepared for *ex vivo* testing as described previously (Brooks and Faulkner, 1988; Hakim et al., 2013). Briefly, the EDL (n=7 *mdm* and 9 wild type) and soleus muscles (n=7 *mdm* and 9 wild type) were surgically exposed, and 4-0 silk sutures were tied to the distal and proximal ends at the muscle–tendon junction, including as little tendon as possible without damaging the muscle fibers. The tendons were cut outside of the suture knots to extract the muscles. Extracted muscles were attached to a dual-mode muscle lever system (Aurora Scientific, Inc., Series 300B, Aurora, ON, Canada). Throughout all experimental protocols, the muscles were bathed in a 21°C Krebs–Henseleit solution containing (in mmol l^{-1}): NaCl (118), KCl (4.75), $MgSO_4$ (1.18), $NaHCO_3$ (24.8), KH_2PO_4 (1.18), $CaCl_2$ (2.54) and glucose (10.0). The bath was aerated with a 95% O_2:5% CO_2 gas mixture. Each muscle was surrounded by two parallel platinum electrodes, which delivered 1 ms square pulses of electrical stimulation at supramaximal voltage (70 mV).

A custom LabVIEW program (National Instruments, Austin, TX, USA) was used to control the lever motor and stimulator. The program also recorded force, length and time at a sampling rate of 4 kHz. After testing, any residual tendinous origins were removed, and the muscle was dabbed dry and weighed. Prior to the experiment, muscles were primed with a 10 s, 1 Hz stimulation train, which decreased the variability of forces measured during the experiment (Hakim et al., 2013).

Muscle force was expressed as stress (N cm^{-2}), calculated as force divided by the physiological cross-sectional area of the muscle. To determine the physiological cross-sectional area, muscle mass was multiplied by the cosine of the pennation angle (Burkholder et al., 1994), and divided by the product of muscle fiber length (Askew and Marsh, 1997; Monroy et al., 2017) and mammalian skeletal muscle density (1.06 g cm^{-3}) (Sacks and Roy, 1982). Fiber lengths were calculated from fiber length:muscle length ratios for *mdm* and wild-type soleus (Monroy et al., 2017) and EDL (0.6; J. Monroy, unpublished data). The ratios are similar to values reported in the literature (Askew and Marsh, 1997).

Mechanical protocol

Twitch contractions were produced using a 1 ms square-wave of electrical stimulation with at least 1 min between stimuli. Maximum twitch stress was found by stimulating each muscle at various lengths until maximum stress was identified at optimal twitch muscle length. From the maximum twitch stress protocol, we measured the three previously defined phases of twitch contractions (Askew and Marsh, 1997; Saladin et al., 2017): (1) EMD, the time (ms) between stimulation and force onset, indicated by a force twice the standard deviation of the electrical noise above the mean passive force; (2) contraction time, the time (ms) between force onset and peak force; and (3) half-relaxation time, the time (ms) between peak force and half maximum force. We also measured the average rate of force development (N cm^{-2} s^{-1}) as the slope of the stress–time relationship during the first 10 ms of the contractile phase.

Finally, we measured the activation dependence of optimal length, defined as the difference in optimal length between twitch and tetanus in units of percent optimal tetanic muscle length (L_0). Upon completion of the twitch protocol (above), the same muscles were used to establish the tetanic force–length relationship. Preliminary experiments indicated that fatigue and damage would prevent muscles from completing the entire protocol. To ensure that muscles could maintain force for the duration of the experiment, we used submaximal stimulation to obtain fused tetanic contractions that produced >90% of maximum stress at optimal length. Tetanic contractions were produced using 80 Hz electrical stimulation until a fused plateau of force was visible with at least 4 min rest between

Journal of Experimental Biology (2019) 222, jeb200840. doi:10.1242/jeb.200840

contractions (Hakim et al., 2013). Maximum tetanic stress was found by stimulating the muscle at different lengths with tetanic stimulation until maximum stress was reached at the tetanic optimal length. A maximum tetanic contraction was performed at the end of the experiment protocol, and if stress was <90% of the original value (indicating fatigue or damage), then the data were discarded.

The lower frequency of stimulation during tetanic contraction may reduce the shift in the force–length relationship between twitch versus tetanic contractions (Holt and Azizi, 2014). Thus, our values are conservative estimates of the activation-dependent shift in the force–length relationship. We also assumed that the force–frequency relationship was similar in wild-type and *mdm* soleus and EDL muscles, as reported for *mdm* diaphragm (Lopez et al., 2008).

Electron microscopy

We measured sarcomere length using a transmission electron microscope. Muscle thickness made other visualization methods, such as light microscopy, impossible. After mechanical experiments, a subset of muscles (EDL tetanus=3 *mdm*, 3 wild type; EDL twitch=3 *mdm*, 4 wild type; soleus tetanus=3 *mdm*, 3 wild type; soleus twitch=3 *mdm*, 4 wild type) were pinned onto corkboard at either tetanic or twitch optimal length with size 00 insect dissection pins while still attached to the lever apparatus to ensure as little change in length as possible. Muscles were fixed with 2.5% glutaraldehyde in sodium cacodylate buffer at 4°C, secondarily fixed with 2% osmium tetroxide in buffer at 25°C, moved through a graded ethanol dehydration series, infiltrated with epoxy resin (catalog no. 14300, Electron Microscopy Sciences, Hartfield, PA, USA), and cured in polyethylene flat embedding molds in an oven at 60°C until hard (~48–72 h).

Muscle blocks were cut into 70 nm ultrathin sections (Reichert-Jung Ultracut E, Buffalo, NY, USA) and placed on copper mesh grids (catalog no. G200-Cu, Electron Microscopy Sciences). Blocks were sectioned to visualize the longitudinal axis of the myofibrils. Grids were stained using UranyLess (catalog no. 22409, Electron Microscopy Sciences) with 0.4% lead citrate, and observed under a transmission electron microscope (JEOL JEM 1200EX II). Sarcomere lengths were analyzed using ImageJ (1.50i, National Institutes of Health, Bethesda, MD, USA). Sarcomere length was defined as the distance between adjacent Z discs along the long axis of the myofibril. To limit effects of uniform sample shrinkage during processing, each picture was scaled to the longitudinal A-band size (1.6 µm) (Al-Khayat, 2013). There is no evidence of a difference in the A-band length, based on TEM images of longitudinal sarcomeres from wild-type and *mdm* triceps surae, as reported by Witt et al. (2004). At least 60 sarcomeres were measured for each muscle over four to eight separate locations within the deep zone of the muscle belly.

Single fibers

Skinned fibers were prepared from *mdm* and wild-type muscles using standard techniques (Joumaa and Herzog, 2014). Muscles were stored in a relaxing solution [in mmol l^{-1}: potassium propionate (170), magnesium acetate (2.5), MOPS (20), K_2EGTA (5) and ATP (2.5), pH 7.0] for 12 h at 4°C, then in a relaxing-glycerol (50:50) solution at −20°C for 4 to 6 weeks (Powers et al., 2017). To limit protein degradation, all solutions contained one tablet of protease inhibitor (Complete, Roche Diagnostics, Mannheim, Germany) per 100 ml of solution.

On the day of the experiments, muscles were rinsed vigorously with relaxing solution to remove glycerol. Washed muscles were dissected into bundles of three to five fibers and were moved to an experimental glass chamber containing relaxing solution for testing (EDL fiber bundles=9 *mdm* from 3 mice, 9 wild type from 4 mice; soleus fiber bundles=10 *mdm* from 3 mice, 8 wild type from 4 mice). One end of the fiber bundle was glued to the hook of a length controller and the other end was glued to the hook of a force transducer (model 400A, Aurora Scientific, Ontario, Canada), allowing for control of fiber length and measurement of force, respectively. After manipulation, each fiber bundle was carefully inspected for damage, and damaged fibers were discarded. Sarcomere length was measured using optical diffraction of an He-Ne laser beam. Recorded forces were expressed as fiber stress (mN mm^{-2}) by dividing force by cross-sectional area of fiber bundles, which was measured using a binocular dissecting

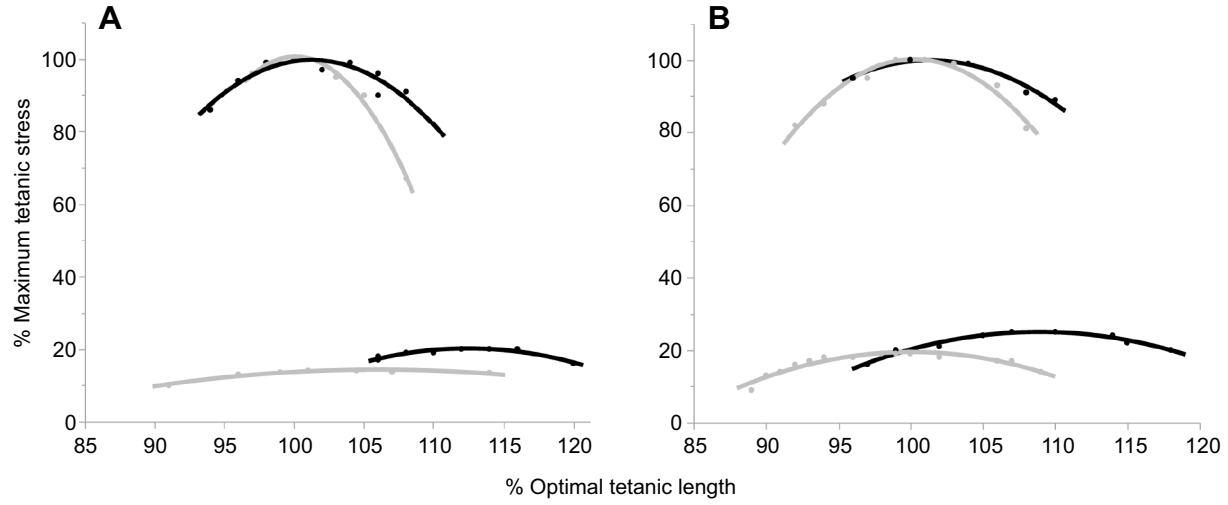

Fig. 1. Representative data set showing the shift in optimal length from twitch to tetanic contractions for individual soleus and extensor digitorum longus (EDL) muscles from a wild-type (black) and a muscular dystrophy with myositis (*mdm*) (gray) mouse. (A) Soleus; (B) EDL. Tetanic stress–length relationships (upper traces) are plotted with respective twitch stress–length relationships (lower traces). Optimal length was determined from the curve fits at each activation level. In wild-type muscles, optimal length is longer for twitch than for tetanic contractions. In contrast, optimal lengths are similar for twitch and tetanic contractions in *mdm* muscles.

Journal of Experimental Biology (2019) 222, jeb200840. doi:10.1242/jeb.200840

microscope at a magnification of 5×, and assuming a cylindrical shape. All experiments were performed at ∼15°C.

Mechanical protocol

To assess length dependence of Ca^{2+} sensitivity, we measured fiber stress at various Ca^{2+} concentrations at short (2.4 µm) and long (3.0 µm) sarcomere lengths. Fibers were moved from relaxing solution into washing solution [in mmol l^{-1}: potassium propionate (185), magnesium acetate (2.5), MOPS (20) and ATP (2.5), pH 7.0] to eliminate EGTA (a Ca^{2+} chelator) previously present in the relaxing solution. Passive fiber stress was recorded at the end of washing. Force–pCa curves were established by moving each fiber through a series of solutions with increasing Ca^{2+} concentrations of pCa 7.0, 6.8, 6.6, 6.4, 6.0, 5.8, 5.4 and 4.2 [in mmol l^{-1}: potassium propionate (170), magnesium acetate (2.5), MOPS (10) and ATP (2.5), and CaEGTA and K_2EGTA were mixed at different proportions to obtain various values of pCa ($-\log[Ca^{2+}]$), pH 7.0]. We previously verified that there was no influence of random or systematic applications of pCa solutions on the force–pCa curves (Joumaa and Herzog, 2014). Fibers were bathed in each solution until a plateau of force was recorded for at least 15 s. Active force was calculated by subtracting the fiber passive force from the total force recorded. For the Ca^{2+}-sensitivity analysis, active force was normalized to the active force produced during supramaximal activation at pCa 4.2 (Joumaa and Herzog, 2014). Force–pCa data were fit to a four-parameter Hill equation (JMP Pro 12.2, SAS Institute, Cary, NC, USA) using standard methods (Walker et al., 2010) to measure the half-maximum force response (pCa50), an indicator of Ca^{2+} sensitivity, and the Hill coefficient (ηH), a measure of actin–myosin cooperativity (Seow, 2013).

Statistical analysis

To assess whether the *mdm* mutation affected soleus and EDL muscles similarly in whole-muscle experiments, we used a full factorial two-way ANOVA, with fixed factors of genotype (wild type, *mdm*), muscle (EDL, soleus) and genotype×muscle interaction. Response variables included electromechanical delay, rate of force development, contraction time, maximum twitch stress, half-relaxation time, maximum tetanic stress, twitch:tetanus ratio, and optimal length shift between twitch and tetanus. To assess whether the *mdm* mutation affected length dependence of Ca^{2+} sensitivity in soleus and EDL fibers, we used a full factorial three-way ANOVA, with main effects of genotype (wild type, *mdm*), muscle (EDL, soleus), sarcomere length (2.4 µm, 3.0 µm), two-way interactions (genotype×muscle, genotype×sarcomere length, muscle×sarcomere length) and three-way interaction (genotype×muscle×sarcomere length). Because individual fibers were used to collect data at both 2.4 and 3.0 µm, we nested individual fibers within genotype as a

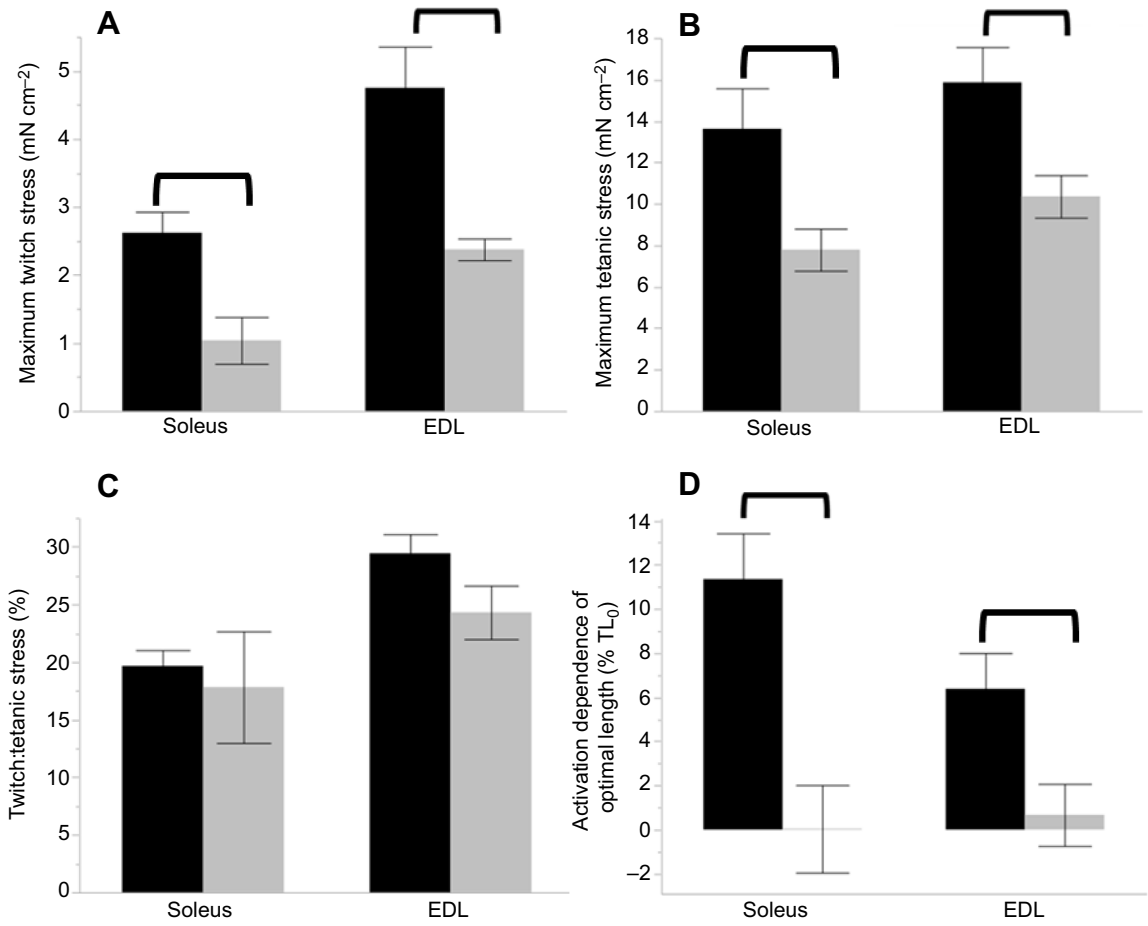

Fig. 2. Maximum stress and optimal length during twitch and tetanic contractions of soleus and EDL muscles from wild-type (black) and *mdm* (gray) mice. (A) Maximum twitch stress was smaller in *mdm* than in wild-type muscles. (B) Maximum tetanic stress was smaller in *mdm* than in wild-type muscles. (C) Ratio of maximum twitch stress to maximum tetanic stress was not significantly different between *mdm* and wild-type muscles. (D) Activation dependence of optimal length between twitch and tetanus was smaller in *mdm* than wild-type muscles. Bracket denotes significant differences between genotypes. For clarity, all other statistics are described in Table 1. Data are means±s.e.m. $\%TL_0$=optimal length difference between twitch and tetanus, normalized to tetanic optimal length.

Journal of Experimental Biology (2019) 222, jeb200840. doi:10.1242/jeb.200840

random effect. Response variables included pCa50, ηH, active stress and passive stress. To assess sarcomere length, we used a full factorial three-way ANOVA with fixed factors of genotype (wild type, *mdm*), activation (tetanus, twitch), muscle (EDL, soleus), all two-way interactions and the three-way interaction. To account for individual variability, we nested individual within genotype as a random effect. To assess sarcomere length variability within EDL and soleus muscles, we used a full factorial two-way ANOVA with fixed factors of genotype (wild type, *mdm*), activation (tetanus, twitch) and genotype×activation interaction.

Alpha values were set at 0.05 and assumptions of normality and homogeneity of variance were evaluated using the Shapiro–Wilk test of normality and Levene's test for equality of variances. A best Box–Cox transformation was used for all data except sarcomere length to meet the assumptions of normality and homoscedasticity; a square root transformation was used for sarcomere length. When model effects were significant, a *post hoc* Tukey's honestly significant difference (HSD) all-pairwise comparison analysis was used to test for differences among group means. The 95% confidence intervals of the means were used to assess whether the twitch optimal length shift in any genotype/muscle group was significantly different from zero. Data are presented as means ±s.e.m. Statistical analysis was conducted using JMP (JMP Pro 12.2, SAS Institute). Although no assumptions were violated for these parametric ANOVA models, because of the relatively small sample size we also conducted a more conservative analysis using non-parametric tests and we report these statistics only if they differed from the parametric results. The non-parametric analysis was done within factors (Wilcoxon ranked test) and in multiple comparisons (Steel–Dwass all pairs).

RESULTS

Wild-type muscles showed the expected pattern of activation dependence of optimal length, with maximal twitch stress produced at a longer muscle length than that of maximal tetanic stress (Bahler et al., 1967; Brown et al., 1999; Holt and Azizi, 2016), whereas *mdm* muscles showed no activation dependence of optimal length (Figs 1 and 2D, Table 1). Furthermore, although the 95% confidence intervals of the means for the activation-dependent shift of optimal length between tetanic and twitch contractions were statistically different from zero in wild-type soleus (95% confidence interval=6.58–16.13 L_0) and EDL (95% confidence interval 3.33–6.40 L_0), they were not statistically different from zero for either *mdm* soleus (95% confidence interval=−3.33–2.40 L_0) or EDL (95% confidence interval −4.35–2.91 L_0), indicating that optimal length is not activation dependent in *mdm* muscles. Maximum twitch stress and maximum tetanic stress were lower in *mdm* muscles compared with wild-type muscles (Fig. 2A,B; Tukey's HSD, $P<0.05$). The ratio between twitch and tetanic maximum stress was similar in wild-type and *mdm* muscles (Fig. 2C; Tukey's HSD, $P<0.05$).

All twitch properties were affected by the *mdm* mutation (Figs 3 and 4, Table 1). EMD was longer in *mdm* than in wild-type muscles, longer in soleus than in EDL in both genotypes, and the *mdm* mutation led to a larger increase in EMD in soleus than EDL (Fig. 4A). Rate of force development was slower in *mdm* than in wild-type muscles, and faster in EDL than soleus (Fig. 4B). Contraction time was longer in soleus than in EDL, longer in *mdm* than in wild-type muscles, and the *mdm* mutation led to a larger increase in contraction time in soleus than in EDL (Fig. 4C). Half-relaxation time was longer in soleus than in EDL, longer in *mdm* than in wild type, and the *mdm* mutation led to a larger increase in half-relaxation time in soleus than in EDL (Fig. 4D).

As measured by electron microscopy, sarcomere lengths differed between genotypes, muscles and activation levels (Fig. 5, Table 2). *Post hoc* analysis (Tukey's HSD, $P<0.05$) indicated that optimal sarcomere length was significantly longer for twitch compared with tetanic activation in wild-type soleus and EDL muscles. However, *mdm* optimal sarcomere lengths did not differ significantly between activation levels or muscles. Furthermore, soleus *mdm* sarcomere length, regardless of activation (tetanic or twitch), was similar to that of wild-type twitch contractions (Fig. 5). For EDL muscles, sarcomere length variability, as measured from TEM images after experiments, was not significantly different between genotypes or

Table 1. Results of two-way ANOVA on twitch properties of wild-type and *mdm* muscles in mice

	Muscle		Genotype		Interaction	
	F	*P*	*F*	*P*	*F*	*P*
tP_0	29.81	<0.0001*	30.74	<0.0001*	1.14	0.29
EMD	73.70	<0.001*	85.57	<0.001*	7.12	0.01*
RFD	48.53	<0.001*	38.40	<0.001*	0.77	0.39
TTP	235.31	<0.001*	65.40	<0.001*	8.19	0.008*
½ RT	140.26	<0.001*	35.80	<0.001*	5.29	0.029*
TP_0	2.16	0.15	11.98	0.0017*	0.010	0.92
ADOL	1.96	0.17	37.89	<0.001*	0.017	0.90
tP_0:TP_0	9.87	0.004*	1.90	0.18	0.30	0.59

tP_0, twitch maximum stress; EMD, electromechanical delay; RFD, rate of force development; TTP, time to peak stress; ½ RT, half relaxation time; TP_0, tetanic maximum stress; ADOL, activation dependence of optimal length, measured as the change in optimal length between tetanic and twitch activation. *$P<0.05$.

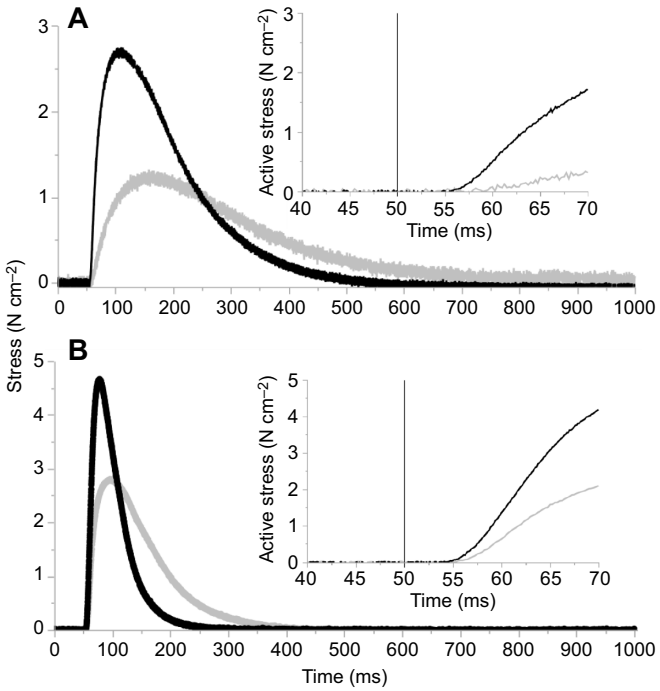

Fig. 3. Representative twitch contractions for soleus and EDL muscles from wild-type (black) and *mdm* (gray) mice. (A) Soleus; (B) EDL. A single 1 ms square-wave of electrical stimulation was applied to muscles at 50 ms. The *mdm* muscles produced a smaller maximum stress and longer duration for all phases of twitch. Inset graphs for soleus (A) and EDL (B) show the electromechanical delay and early force rise, with stimulation indicated by a vertical line.

Journal of Experimental Biology (2019) 222, jeb200840. doi:10.1242/jeb.200840

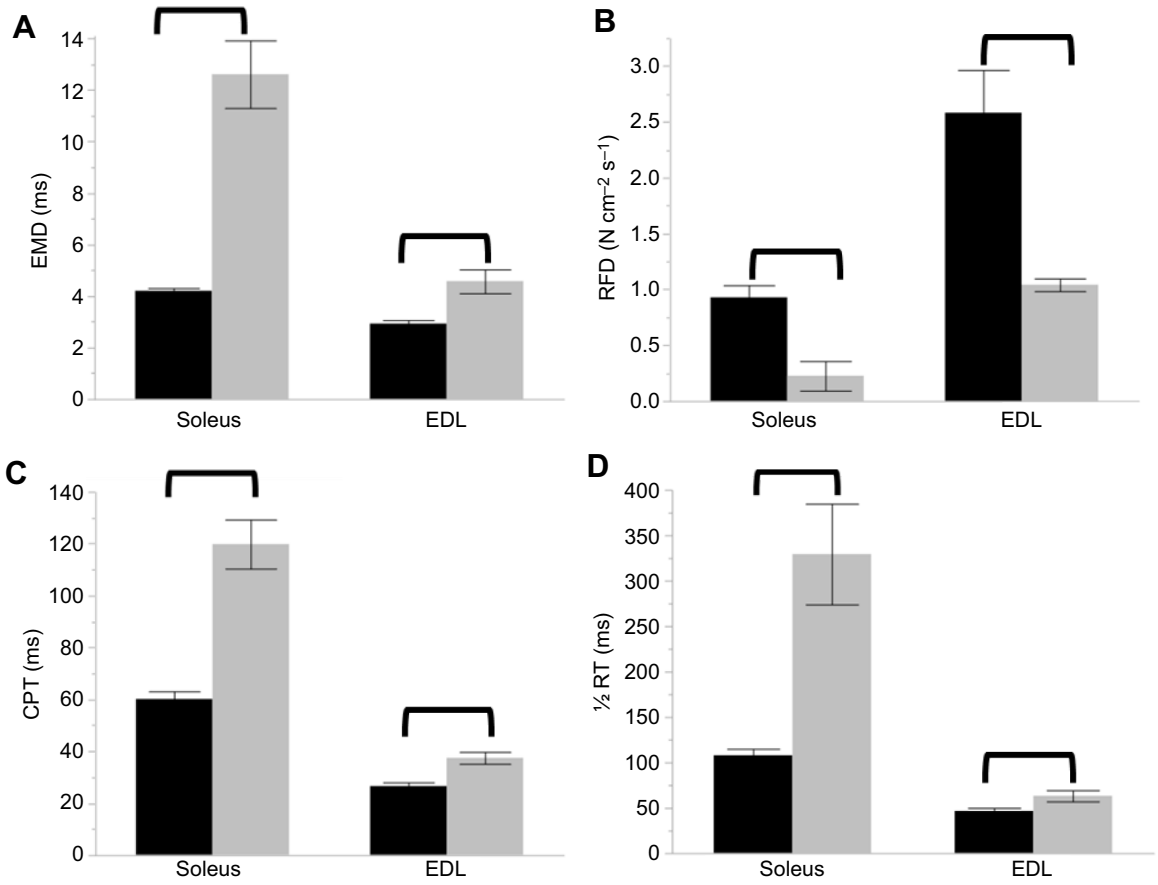

Fig. 4. Characteristics of twitch contractions for soleus and EDL muscles from wild-type (black) and *mdm* (gray) mice. (A) Electromechanical delay was longer in *mdm* than in wild-type muscles, and the *mdm* mutation led to a larger increase in electromechanical delay in soleus than in EDL. (B) Rate of force development was slower in *mdm* than in wild type. (C) Contraction time was longer in soleus than in EDL, longer in *mdm* than in wild type, and the *mdm* mutation led to a larger increase in contraction time in soleus than in EDL. (D) Half-relaxation time was longer in soleus than in EDL, longer in *mdm* than in wild type, and the *mdm* mutation led to a larger increase in half-relaxation time in soleus than EDL. Bracket denotes significant differences between genotypes. For clarity, all other statistics are described in Table 1. Data are means±s.e.m. EMD, electromechanical delay; RFD, rate of force development; CT, contraction time; ½ RT, half-relaxation time.

activation conditions. In contrast, sarcomere length variability for soleus muscles was significantly smaller in twitch versus tetanic conditions (Tukey's HSD, $P<0.05$), regardless of genotype.

Length dependence of Ca^{2+} sensitivity was similar between genotypes (Figs 6 and 7, Table 3). Force–pCa data from fiber bundles were well fit by the Hill equation ($r^2<0.90$; Fig. 6). Force–pCa curves of *mdm* and wild-type soleus fibers were similar at both sarcomere lengths (Fig. 6A), except for the upper asymptote of *mdm* soleus at 3.0 µm (Fig. 6A lower traces). EDL *mdm* and wild-type force–pCa curves were similar at both sarcomere lengths. pCa50 was larger at 3.0 µm than at 2.4 µm in *mdm* and wild-type soleus and EDL muscles (Tukey's HSD, $P<0.05$). The Hill coefficient, ηH, was larger in EDL than in soleus fibers (Tukey's HSD, $P<0.05$). *Mdm* soleus fibres produced less active stress than wild-type soleus fibres, active stress was lower at 3.0 µm than at 2.4 µm, and active stress was larger in EDL than in soleus fibres (Tukey's HSD, $P<0.05$). At 2.4 µm, passive stress was similar between *mdm* and wild type and between EDL and soleus fibres (Tukey's HSD, $P<0.05$). At 3.0 µm, passive stress was larger in *mdm* than in wild type for both muscles, and passive stress was larger in soleus than in EDL (Tukey's HSD, $P<0.05$). However, this difference was not statistically significant in the non-parametric assessment (Steel–Dwass all pairs, $P=0.12$).

DISCUSSION

Activation dependence of optimal length and length dependence of Ca^{2+} sensitivity

The observation that optimal muscle length decreases at higher compared with lower activation levels in skeletal muscles (Bahler et al., 1967; Close, 1972; Holt and Azizi, 2014; Prasartwuth et al., 2006) was confirmed for wild-type EDL and soleus. Compared with tetanic activation, optimal lengths of ∼106% and ∼111% L_0 were observed during twitch activation of EDL and soleus, respectively. In contrast, there was no difference in optimal length between tetanic and twitch contractions in *mdm* EDL or soleus.

Activation dependence of optimal length is thought to be linked to length-dependent activation (McDonald et al., 1997; Rassier et al., 1999). Because we found no activation dependence of optimal length in *mdm* muscles, we also assessed length dependence of activation as measured by Ca^{2+} sensitivity in fibre bundles. There was no difference in Ca^{2+} sensitivity or length dependence of Ca^{2+} sensitivity between wild-type and *mdm* fibres. This observation contradicts the hypothesis that there is a causal link between length-dependent activation and activation dependence of optimal length. At least, length dependence of Ca^{2+} sensitivity alone does not appear sufficient to produce activation dependence of optimal muscle length.

Journal of Experimental Biology (2019) 222, jeb200840. doi:10.1242/jeb.200840

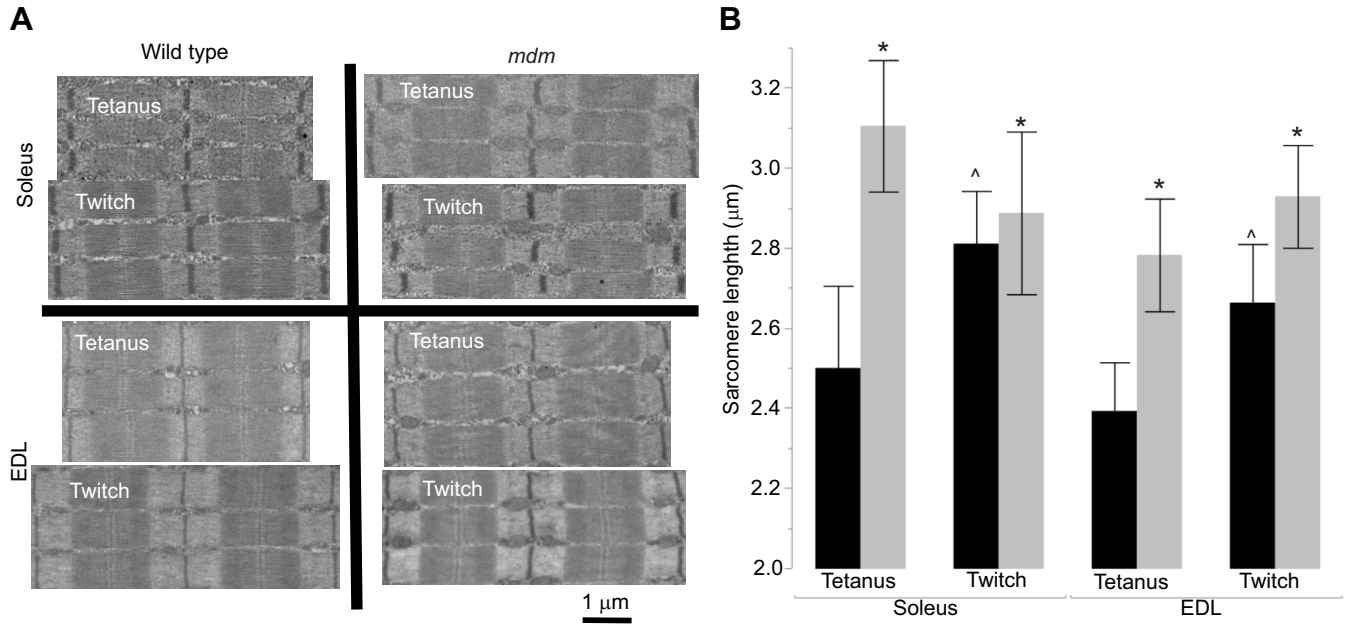

Fig. 5. Optimal sarcomere length of soleus and EDL muscles from wild-type (black) and *mdm* (gray) mice. (A) Representative TEM images of soleus and EDL muscle from wild-type and *mdm* mice, which were fixed in passive muscle pinned at optimal tetanic or twitch muscle length. The optimal sarcomere length during twitch was larger than tetanic activation in wild-type soleus and EDL muscles. The optimal sarcomere lengths of *mdm* soleus and EDL muscles were the same for tetanic and twitch activations. *Significantly different from wild type under same condition; ^statistically different from wild-type tetanic activation. Bars are means±s.e.m.

The molecular mechanisms that underlie length dependence of Ca^{2+} sensitivity remain unknown (de Tombe et al., 2010; MacIntosh, 2017; Rassier et al., 1999). One historical argument was that length dependence of Ca^{2+} sensitivity is caused by an increase in cross-bridge binding rates that results from reduced lattice spacing at longer, compared with shorter, sarcomere lengths (de Tombe et al., 2010; Rassier et al., 1999). However, a role for lattice spacing now appears limited. For example, Konhilas et al. (2002a) found that changes in lattice spacing with stretch were not sufficient to explain the length-dependent increase in Ca^{2+} sensitivity.

Current theories have focused instead on length-dependent thick and/or thin filament cooperativity (Fukuda et al., 2011; Terui et al., 2010). Cross-bridge attachment to the thin filaments may be facilitated by neighboring cross-bridges that are already attached, the so-called ‘thick filament cooperativity’ (Fusi et al., 2016; Linari et al., 2015; Reconditi et al., 2014). This property is predicted to increase with increasing sarcomere length owing to length-dependent strain of the thick filament. Increasing filament strain is thought to increase thick filament cooperativity (Fusi et al., 2016; Linari et al., 2015). Additionally, tropomyosin activation may be facilitated by neighboring troponin complexes that are already active, the so-called ‘thin filament cooperativity’ (Fukuda et al., 2011; Terui et al., 2008), which increases with increasing sarcomere length (Fukuda et al., 2011; Terui et al., 2008). We found no difference in length dependence of calcium sensitivity between wild-type and *mdm* muscles, suggesting no effect of the *mdm* mutation regardless of the mechanisms involved.

Table 2. Results of three-way ANOVA for differences in sarcomere length between genotypes and muscles

Source	*F*	*P*
Genotype	48.57	<001*
Muscle	4.76	0.04*
Activation	9.74	0.005*
Genotype×Muscle	0.12	0.73
Genotype×Activation	13.56	0.001*
Muscle×Activation	1.87	0.19
Genotype×Muscle×Activation	4.68	0.04*

*P<0.05.

Few studies have suggested alternative mechanisms for activation dependence of optimal muscle length. Holt and Azizi (2014) found that optimal muscle length during submaximal activation was not related to Ca^{2+} levels inferred from the method of stimulation. Although they identified no specific mechanism, they suggested that absolute force was related to optimal length owing to activation-dependent interactions between cross-bridges and the force transmission system (Holt and Azizi, 2014). In contrast, MacNaughton et al. (2007) reported that activation dependence of optimal length between twitch and tetanus during submaximal contractions was unaffected by dantrolene, which reduces Ca^{2+} release and intracellular [Ca^{2+}] as well as force. This finding contradicts the idea that absolute force per se is involved in activation dependence of optimal length.

During fixed-end contractions, muscle fibres shorten against series elastic elements even though the total length remains constant (Bahler et al., 1967; Holt and Williams, 2018; Street et al., 1966). Similar to Holt and Azizi (2014), Bahler et al. (1967) suggested that optimal muscle length should be longer in twitch than in tetanic contractions because fiber shortening increases with increasing force. In a preliminary study using video microscopy, intact wild-type soleus muscles were observed to shorten by ∼4% during tetanic contractions and by ∼1% during twitch contractions, whereas shortening during both tetanic and twitch contractions was negligible in *mdm* soleus muscles (J. Monroy, personal observations). In contracting wild-type soleus muscles, the expected shift in optimal sarcomere length between tetanic and

Journal of Experimental Biology (2019) 222, jeb200840. doi:10.1242/jeb.200840

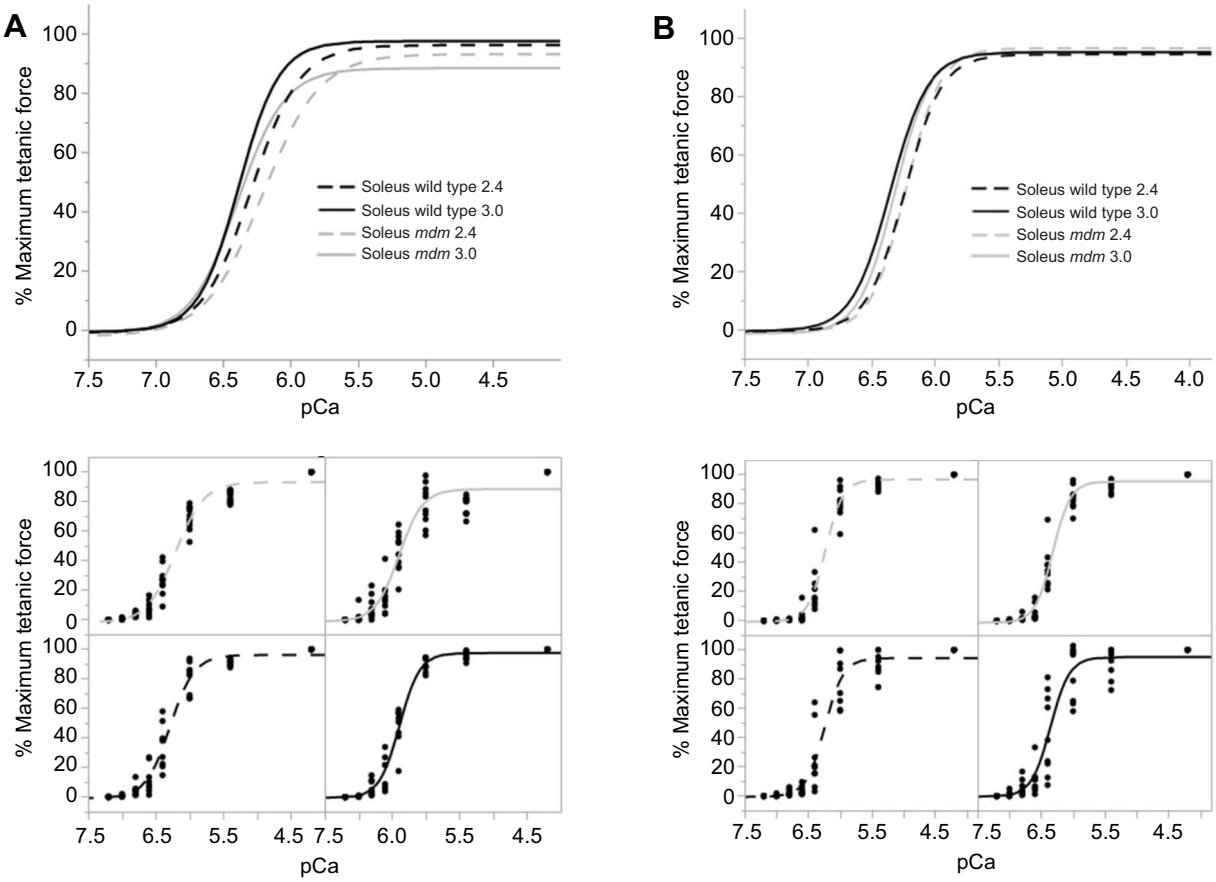

Fig. 6. Length dependence of Ca^{2+} sensitivity of soleus and EDL fiber bundles from wild-type (black) and mdm (gray) mice. (A) Soleus; (B) EDL. Ca^{2+} sensitivity relationships at sarcomere lengths of 2.4 (dashed lines) and 3.0 µm (solid lines) from wild-type and *mdm* fibre bundles (top). Individual data points for each curve are shown below. The shift in Ca^{2+} sensitivity from 2.4 to 3.0 µm was similar between genotypes.

twitch contractions owing to fiber shortening is only ∼3% (versus 11% observed at the whole muscle level), whereas no length-dependent shift in optimal sarcomere length is expected for *mdm* soleus, as indeed was observed. This analysis suggests that fiber shortening during isometric contraction is too small to account for the relatively much shorter lengths found during tetanic contraction of wild-type muscles compared with twitch contraction.

Optimal tetanic muscle length need not occur at the same absolute sarcomere lengths in wild-type and *mdm* muscles. Because optimal muscle lengths are similar for twitch and tetanic contractions in *mdm* muscles, it is not clear whether this sarcomere length corresponds to twitch or tetanic sarcomere lengths of wild-type muscles, or possibly is somewhere in between. For wild-type muscles, tetanic sarcomere lengths corrected for shortening during force development would be ∼2.40 and ∼2.29 µm for soleus and EDL, respectively, and twitch sarcomere lengths would be ∼2.78 and ∼2.63 µm for soleus and EDL, respectively. These data suggest that sarcomere lengths of *mdm* muscles during both tetanic and twitch contractions were even longer than for wild-type twitch contractions before correcting for shortening during force development.

Why is tetanic optimal sarcomere length longer in *mdm* muscles? One possible explanation is that *mdm* sarcomeres are structurally unstable at optimal filament overlap and become more stable at longer lengths. Selectively degrading titin reduces force almost linearly (Horowits et al., 1986; Li et al., 2018) and leads to positional instability of thick filaments (Horowits, 1992; Horowits and Podolsky, 1988). Therefore, it is possible that decreased stiffness of titin in *mdm* muscles, as measured by the slope of the stress versus strain curve during long stretches (Powers et al., 2016, 2017), decreases sarcomere stability at shorter sarcomere lengths. However, at longer sarcomere lengths, titin bears more force (Linke et al., 1998; Trombitás et al., 1998), which may help to stabilize the sarcomeres.

The longer sarcomere lengths of *mdm* muscles at tetanic optimum length suggest that reduction in filament overlap could also contribute to reduced contractile stress. Contractile stress was estimated at each sarcomere length by assuming a linear force–length relationship from maximum stress at 2.5 µm to zero stress at 4.0 µm. Owing to the difference in sarcomere lengths estimated above, maximum tetanic stress would be reduced by ∼11.3% and ∼20.7% for *mdm* EDL and soleus, respectively, compared with wild-type muscles. For comparison, the measured reduction in tetanic stress in *mdm* EDL and soleus was 37.8% and 44.2%, respectively. Thus, the reduction in filament overlap accounts for at most ∼30–47% of the observed difference. This is a liberal estimate because fixed-end contractions have a more curved force–length relationship (Pollack, 1990; Rassier et al., 1999), which means that force on the descending limb is likely underestimated.

The Ca^{2+} sensitivity tests were conducted at sarcomere lengths of 2.4 and 3.0 µm for both *mdm* and wild-type muscles using standard procedures (Mateja et al., 2013). According to the TEM results, optimal muscle lengths corresponded to optimal sarcomere lengths of 3.0 µm in *mdm* muscles and 2.4 µm in wild-type muscles. This suggests that the calcium sensitivity may have been tested at different regions of the force–length relationship in the *mdm* and

Journal of Experimental Biology (2019) 222, jeb200840. doi:10.1242/jeb.200840

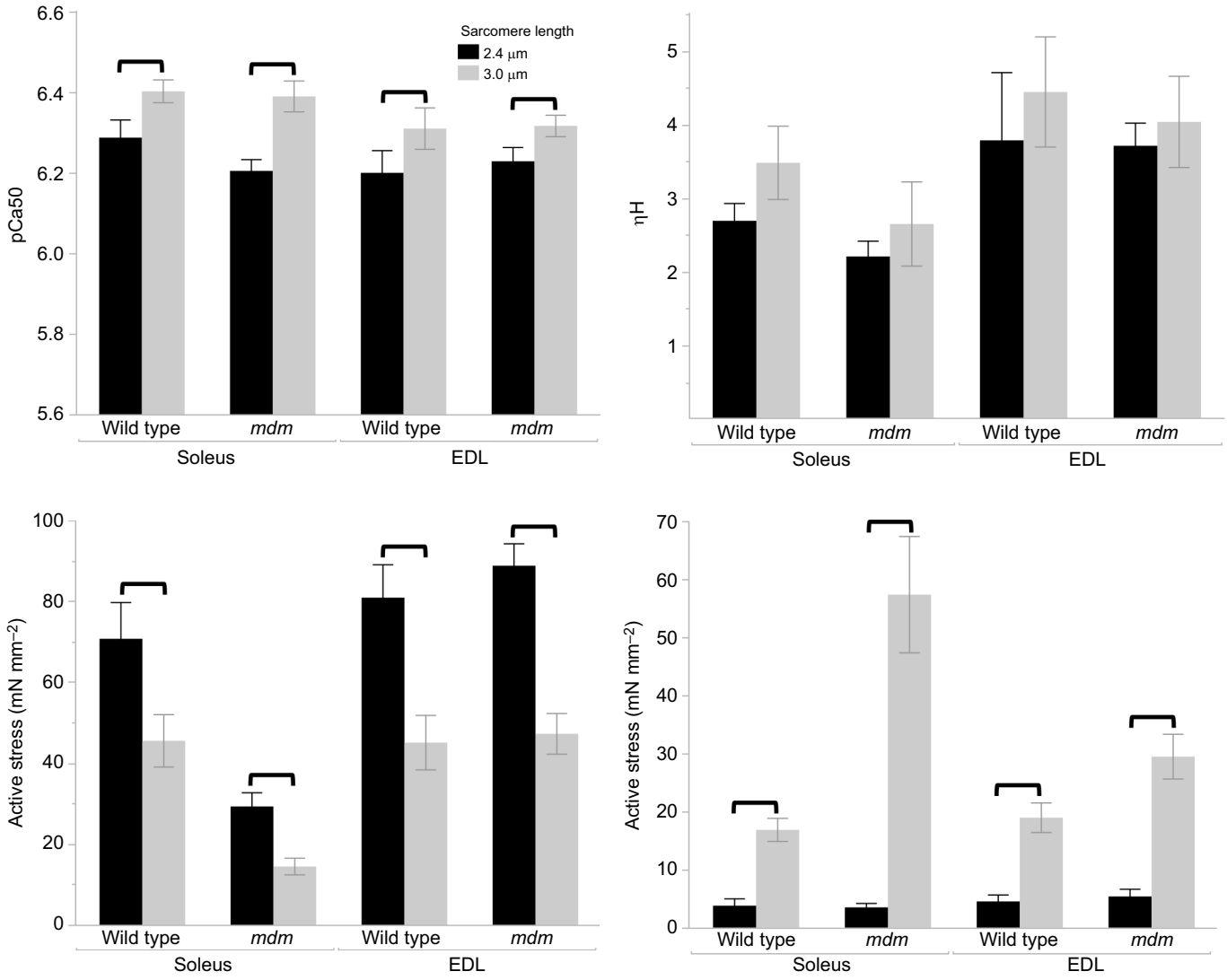

Fig. 7. Half-maximum force response (pCa50) and Hill coefficient (ηH) of soleus and EDL fiber bundles from wild-type (black) and *mdm* (gray) mice. (A) pCa50 was larger in fibres at 3.0 µm than at 2.4 µm. (B) ηH was not significantly different between *mdm* and wild type for either length or muscle type. (C) Active stress was lower in *mdm* than in wild type for soleus only. (D) Passive stress was larger at 3.0 µm than at 2.4 µm, and larger in *mdm* than in wild type for soleus and EDL muscles at a sarcomere length of 3.0 µm. Bracket denotes significant differences between sarcomere lengths. For clarity, all other statistics are described in Table 3. Data are means±s.e.m.

wild-type muscles. Therefore, we cannot rule out the possibility that a Ca^{2+} sensitivity shift might occur in *mdm* muscles at sarcomere lengths longer than 3.0 µm. However, optimal muscle length was obtained by activating the whole muscle at increasing lengths until the maximal force was reached, then the muscle was fixed and sarcomere lengths were determined using TEM. Knowing that maximal force of the whole muscle depends not only on the sarcomere lengths, but also on many other parameters such as the architecture of the muscle, sarcomere length non-uniformities between fibers, and the level of activation, a shift in the optimal muscle length does not necessarily mean a shift in the force–sarcomere length relationship at the level of fibers. Further research is warranted to elucidate the force–sarcomere length relationship at the single-fiber level in *mdm* and wild-type fibers.

Isometric force characteristics of *mdm* muscles

We found that *mdm* muscles exhibited a prolonged electromechanical delay, prolonged contraction and half-relaxation times, slower rate of force development, and smaller twitch and tetanic maximum stress compared with wild-type muscles. Force production results from numerous mechanisms including Ca^{2+} release and reuptake (Reddish et al., 2017), actin–myosin kinetics (Gordon et al., 2000; Guellich et al., 2014; Schiaffino and Reggiani, 1994) and force transmission (Bloch and Gonzalez-Serratos, 2003; Hughes et al., 2015; Monti et al., 1999; Patel and Lieber, 1997), any or all of which could be affected, directly or indirectly, by the *mdm* mutation. However, the present and other studies found that in skinned fibres and myofibrils where calcium activation is controlled experimentally (e.g. Powers et al., 2016), differences in active stress between genotypes persist. Therefore, it appears unlikely that changes in Ca^{2+} handling alone are responsible for the reduced active force of *mdm* muscles. Furthermore, a major change in myosin heavy chain isoform expression appears unlikely because there were no differences in twitch:tetanus ratio (mean twitch:tetanus ratio was 0.18 for soleus and 0.26 for EDL) or maximum shortening velocity (U. Tahir, unpublished data) between genotypes. It is possible that force

Journal of Experimental Biology (2019) 222, jeb200840. doi:10.1242/jeb.200840

Table 3. Results of three-way ANOVA for Ca^{2+}-sensitivity analysis

	SL		Genotype		Muscle		Genotype×SL		Muscle×Genotype		Muscle×SL		Muscle×SL×Genotype	
	F	*P*	*F*	*P*	*F*	*P*	*F*	*P*	*F*	*P*	*F*	*P*	*F*	*P*
pCa50	22.39	<0.001*	0.23	0.64	4.40	0.04*	0.26	0.61	1.22	0.27	1.06	0.31	0.72	0.40
ηH	0.46	0.50	1.36	0.26	11.59	<0.001*	0.29	0.59	1.75	0.19	0.12	0.74	0.17	0.69
Active	47.75	<0.001*	18.09	<0.001	40.34	<0.001*	31.19	<0.001*	31.19	<0.001*	1.96	0.17	0.03	0.86
Passive	182.91	<0.001*	15.93	<0.001*	0.14	0.71	8.92	<0.001*	2.18	0.15	4.67	0.03*	3.31	0.07*

SL, sarcomere length; pCa50, Ca^{2+} concentration at half maximum force; ηH, Hill coefficient (index of cooperativity); passive, passive stress; active, active stress. *P<0.05.

transmission may be compromised in *mdm* muscles. *Mdm* muscles exhibited a longer electromechanical delay, decreased rate of force development, increased relaxation time, and decreased active stress.

A decrease in series elastic stiffness by increased tendon length would be consistent with these results (Bahler et al., 1967; Mayfield et al., 2016). However, *mdm* muscle preparations in this study had little to no tendon, but do show an increase in endomysial and perimysial connective tissue (Lopez et al., 2008; Powers et al., 2017), and have altered elastic properties that are consistent with greater compliance of active muscle (Monroy et al., 2017). However, internal aponeuroses or internal extracellular matrix components of muscles are not mechanistically (based on Hill-type muscle models) in-series with active fibres, but in-parallel, and thus will have no effect on force transmission.

Conclusions

In contrast to wild-type muscles, *mdm* muscles show no activation dependence of optimal muscle length, yet the length dependence of Ca^{2+} sensitivity was similar in wild-type and *mdm* muscles. This observation suggests that factors other than length dependence of Ca^{2+} sensitivity are likely responsible for activation dependence of optimal length. *Mdm* muscles produced maximum tetanic stress during sub-optimal filament overlap at lengths similar to twitch contractions, but the difference explains less than half of the observed reduction in active force of *mdm* muscles. All twitch characteristics were prolonged in *mdm* compared with wild-type muscles, suggesting a decrease in the rate of force development. The mechanism remains to be elucidated.

Acknowledgements

We thank S. Lindstedt, J. Monroy, N. Holt, and B. Raiteri for improving earlier versions of this manuscript.

Competing interests

The authors declare no competing or financial interests.

Author contributions

Conceptualization: A.L.H.; Methodology: A.L.H., V.J., S.E., K.C.N.; Formal analysis: A.L.H.; Investigation: A.L.H., V.J., S.E.; Resources: K.C.N.; Data curation: A.L.H.; Writing - original draft: A.L.H., S.E.; Writing - review & editing: A.L.H., V.J., S.E., W.H., K.C.N.; Visualization: S.E., K.C.N.; Supervision: V.J., W.H., K.C.N.; Funding acquisition: W.H., K.C.N.

Funding

This work was supported by the National Science Foundation [IOS-0732949, IOS-1025806 and IOS-1456868 to K.C.N.], the W. M. Keck Foundation [K.C.N.], and the Achievement Rewards for College Scientists Foundation [A.L.H.].

References

Al-Khayat, H. A. (2013). Three-dimensional structure of the human myosin thick filament: clinical implications. *Glob. Cardiol. Sci. Pract.* **2013**, 280-302. doi:10.5339/qfarf.2013.BIOP-073

Askew, G. N. and Marsh, R. L. (1997). The effects of length trajectory on the mechanical power output of mouse skeletal muscles. *J. Exp. Biol.* **200**, 3119-3131.

Bahler, A. S., Fales, J. T. and Zierler, K. L. (1967). The active state of mammalian skeletal muscle. *J. Gen. Physiol.* **50**, 2239-2253. doi:10.1085/jgp.50.9.2239

Bloch, R. J. and Gonzalez-Serratos, H. (2003). Lateral force transmission across costameres in skeletal muscle. *Exerc. Sport Sci. Rev.* **31**, 73-78. doi:10.1097/00003677-200304000-00004

Brooks, S. V. and Faulkner, J. A. (1988). Contractile properties of skeletal muscles from young, adult and aged mice. *J. Physiol.* **404**, 71-82. doi:10.1113/jphysiol.1988.sp017279

Brown, I. E., Cheng, E. J. and Loeb, G. E. (1999). Measured and modeled properties of mammalian skeletal muscle. II. The effects of stimulus frequency on force–length and force–velocity relationships. *J. Muscle Res. Cell Motil.* **20**, 627-643. doi:10.1023/A:1005585030764

Burkholder, T. J., Fingado, B., Baron, S. and Lieber, R. L. (1994). Relationship between muscle fiber types and sizes and muscle architectural properties in the mouse hindlimb. *J. Morphol.* **221**, 177-190. doi:10.1002/jmor.1052210207
Close, R. I. (1972). The relations between sarcomere length and characteristics of isometric twitch contractions of frog sartorius muscle. *J. Physiol.* **220**, 745-762. doi:10.1113/jphysiol.1972.sp009733
de Tombe, P. P., Mateja, R. D., Tachampa, K., Ait Mou, Y., Farman, G. P. and Irving, T. C. (2010). Myofilament length dependent activation. *J. Mol. Cell Cardiol.* **48**, 851-858. doi:10.1016/j.yjmcc.2009.12.017
Dutta, S., Tsiros, C., Sundar, S. L., Athar, H., Moore, J., Nelson, B., Gage, M. J. and Nishikawa, K. (2018). Calcium increases titin N2A binding to F-actin and regulated thin filaments. *Sci. Rep.* **8**, 14575. doi:10.1038/s41598-018-32952-8
Freiburg, A., Trombitas, K., Hell, W., Cazorla, O., Fougerousse, F., Centner, T., Kolmerer, B., Witt, C., Beckmann, J. S., Gregorio, C. C. et al. (2000). Series of exon-skipping events in the elastic spring region of titin as the structural basis for myofibrillar elastic diversity. *Circ. Res.* **86**, 1114-1121. doi:10.1161/01.RES.86.11.1114
Fukuda, N., Inoue, T., Yamane, M., Terui, T., Kobirumaki, F., Ohtsuki, I., Ishiwata, S. and Kurihara, S. (2011). Sarcomere length-dependent Ca^{2+} activation in skinned rabbit psoas muscle fibers: coordinated regulation of thin filament cooperative activation and passive force. *J. Physiol. Sci.* **61**, 515-523. doi:10.1007/s12576-011-0173-8
Fusi, L., Brunello, E., Yan, Z. and Irving, M. (2016). Thick filament mechano-sensing is a calcium-independent regulatory mechanism in skeletal muscle. *Nat. Commun.* **7**, 13281. doi:10.1038/ncomms13281
Garvey, S. M., Rajan, C., Lerner, A. P., Frankel, W. N. and Cox, G. A. (2002). The muscular dystrophy with myositis (*mdm*) mouse mutation disrupts a skeletal muscle-specific domain of titin. *Genomics* **79**, 146-149. doi:10.1006/geno.2002.6685
Gordon, A. M., Huxley, A. F. and Julian, F. J. (1966). The variation in isometric tension with sarcomere length in vertebrate muscle fibres. *J. Physiol.* **184**, 170-192. doi:10.1113/jphysiol.1966.sp007909
Gordon, A. M., Homsher, E. and Regnier, M. (2000). Regulation of contraction in striated muscle. *Physiol. Rev.* **80**, 853-924. doi:10.1152/physrev.2000.80.2.853
Guellich, A., Negroni, E., Decostre, V., Demoule, A. and Coirault, C. (2014). Altered cross-bridge properties in skeletal muscle dystrophies. *Front. Physiol.* **5**, 393. doi:10.3389/fphys.2014.00393
Gulati, J., Sonnenblick, E. and Babu, A. (1991). The role of troponin C in the length dependence of Ca^{2+}-sensitive force of mammalian skeletal and cardiac muscles. *J. Physiol.* **441**, 305-324. doi:10.1113/jphysiol.1991.sp018753
Hakim, C. H., Wasala, N. B. and Duan, D. (2013). Evaluation of muscle function of the extensor digitorum longus muscle *ex vivo* and tibialis anterior muscle *in situ* in mice. *J. Vis. Exp.* **9**, 50183. doi:10.3791/50183
Holt, N. C. and Azizi, E. (2014). What drives activation-dependent shifts in the force–length curve? *Biol. Lett.* **10**, 20140651-20140651. doi:10.1098/rsbl.2014.0651
Holt, N. C. and Azizi, E. (2016). The effect of activation level on muscle function during locomotion: are optimal lengths and velocities always used? *Proc. Biol. Sci.* **283**, 20152832. doi:10.1098/rspb.2015.2832
Holt, N. C. and Williams, C. D. (2018). Can strain dependent inhibition of cross-bridge binding explain shifts in optimum muscle length? *Integr. Comp. Biol.* **58**, 174-185. doi:10.1093/icb/icy050
Horowits, R. (1992). Passive force generation and titin isoforms in mammalian skeletal muscle. *Biophys. J.* **61**, 392-398. doi:10.1016/S0006-3495(92)81845-3
Horowits, R. and Podolsky, R. J. (1988). Thick filament movement and isometric tension in activated skeletal muscle. *Biophys. J.* **54**, 165-171. doi:10.1016/S0006-3495(88)82941-2
Horowits, R., Kempner, E. S., Bisher, M. E. and Podolsky, R. J. (1986). A physiological role for titin and nebulin in skeletal muscle. *Nature* **323**, 160-164. doi:10.1038/323160a0
Hughes, D. C., Wallace, M. A. and Baar, K. (2015). Effects of aging, exercise, and disease on force transfer in skeletal muscle. *Am. J. Physiol. Endocrinol. Metab.* **309**, E1-E10. doi:10.1152/ajpendo.00095.2015
Huxley, H. E. (1957). The double array of filaments in cross-striated muscle. *J Biophys Biochem Cytol* **3**, 631-648. doi:10.1083/jcb.3.5.631
Huxley, H. and Hanson, J. (1954). Changes in the cross-striations of muscle during contraction and stretch and their structural interpretation. *Nature* **173**, 973-976. doi:10.1038/173973a0
Huxley, A. F. and Niedergerke, R. (1954). Structural changes in muscle during contraction; interference microscopy of living muscle fibres. *Nature* **173**, 971-973. doi:10.1038/173971a0
Joumaa, V. and Herzog, W. (2014). Calcium sensitivity of residual force enhancement in rabbit skinned fibers. *Am. J. Physiol. Cell Physiol.* **307**, C395-C401. doi:10.1152/ajpcell.00052.2014
Joumaa, V., Rassier, D. E., Leonard, T. R. and Herzog, W. (2007). Passive force enhancement in single myofibrils. *Pflugers Arch.* **455**, 367-371. doi:10.1007/s00424-007-0287-2
Joumaa, V., Rassier, D. E., Leonard, T. R. and Herzog, W. (2008). The origin of passive force enhancement in skeletal muscle. *Am. J. Physiol. Cell Physiol.* **294**, C74-C78. doi:10.1152/ajpcell.00218.2007
Konhilas, J. P., Irving, T. C. and de Tombe, P. P. (2002a). Myofilament calcium sensitivity in skinned rat cardiac trabeculae: role of interfilament spacing. *Circ. Res.* **90**, 59-65. doi:10.1161/hh0102.102269
Konhilas, J. P., Irving, T. C. and de Tombe, P. P. (2002b). Length-dependent activation in three striated muscle types of the rat. *J. Physiol.* **544**, 225-236. doi:10.1113/jphysiol.2002.024505
Kushmerick, M. J., Moerland, T. S. and Wiseman, R. W. (1992). Mammalian skeletal muscle fibers distinguished by contents of phosphocreatine, ATP, and Pi. *Proc. Natl. Acad. Sci. USA* **89**, 7521-7525. doi:10.1073/pnas.89.16.7521
Labeit, D., Watanabe, K., Witt, C., Fujita, H., Wu, Y., Lahmers, S., Funck, T., Labeit, S. and Granzier, H. (2003). Calcium-dependent molecular spring elements in the giant protein titin. *Proc. Natl. Acad. Sci. USA* **100**, 13716-13721. doi:10.1073/pnas.2235652100
Leonard, T. R. and Herzog, W. (2010). Regulation of muscle force in the absence of actin-myosin-based cross-bridge interaction. *Am. J. Physiol. Cell Physiol.* **299**, C14-C20. doi:10.1152/ajpcell.00049.2010
Li, Y., Unger, A., von Frieling-Salewsky, M., Rivas Pardo, J. A., Fernandez, J. M. and Linke, W. A. (2018). Quantifying the titin contribution to muscle force generation using a novel method to specifically cleave the titin springs *in situ*. *Biophys. J.* **114**, 645a. doi:10.1016/j.bpj.2017.11.3480
Linari, M., Brunello, E., Reconditi, M., Fusi, L., Caremani, M., Narayanan, T., Piazzesi, G., Lombardi, V. and Irving, M. (2015). Force generation by skeletal muscle is controlled by mechanosensing in myosin filaments. *Nature* **528**, 276-279. doi:10.1038/nature15727
Linke, W. A. (2017). Titin gene and protein functions in passive and active muscle. *Annu. Rev. Physiol.* **80**, 389-411. doi:10.1146/annurev-physiol-021317-121234
Linke, W. A., Stockmeier, M. R., Ivemeyer, M., Hosser, H. and Mundel, P. (1998). Characterizing titin's I-band Ig domain region as an entropic spring. *J. Cell Sci.* **111**, 1567-1574.
Lopez, M. A., Pardo, P. S., Cox, G. A. and Boriek, A. M. (2008). Early mechanical dysfunction of the diaphragm in the muscular dystrophy with myositis (Ttnmdm) model. *Am. J. Physiol. Cell Physiol.* **295**, C1092-C1102. doi:10.1152/ajpcell.16.2008
Ma, W., Gong, H., Kiss, B., Lee, E.-J., Granzier, H. and Irving, T. (2018). Thick-filament extensibility in intact skeletal muscle. *Biophys. J.* **115**, 1580-1588. doi:10.1016/j.bpj.2018.08.038
MacIntosh, B. R. (2017). Recent developments in understanding the length dependence of contractile response of skeletal muscle. *Eur. J. Appl. Physiol.* **117**, 1059-1071. doi:10.1007/s00421-017-3591-3
MacNaughton, M. B., Campbell, J. J. and MacIntosh, B. R. (2007). Dantrolene, like fatigue, has a length-dependent effect on submaximal force-length relationships of rat gastrocnemius muscle. *Acta Physiol. (Oxf.)* **189**, 271-278. doi:10.1111/j.1748-1716.2006.01645.x
Mateja, R. D., Greaser, M. L. and de Tombe, P. P. (2013). Impact of titin isoform on length dependent activation and cross-bridge cycling kinetics in rat skeletal muscle. *Biochim. Biophys. Acta* **1833**, 804-811. doi:10.1016/j.bbamcr.2012.08.011
Mayfield, D. L., Launikonis, B. S., Cresswell, A. G. and Lichtwark, G. A. (2016). Additional in-series compliance reduces muscle force summation and alters the time course of force relaxation during fixed-end contractions. *J. Exp. Biol.* **219**, 3587-3596. doi:10.1242/jeb.143123
McDonald, K. S., Wolff, M. R. and Moss, R. L. (1997). Sarcomere length dependence of the rate of tension redevelopment and submaximal tension in rat and rabbit skinned skeletal muscle fibres. *J. Physiol.* **501**, 607-621. doi:10.1111/j.1469-7793.1997.607bm.x
Monroy, J. A., Powers, K. L., Pace, C. M., Uyeno, T. and Nishikawa, K. C. (2017). Effects of activation on the elastic properties of intact soleus muscles with a deletion in titin. *J. Exp. Biol.* **220**, 828-836. doi:10.1242/jeb.139717
Monti, R. J., Roy, R. R., Hodgson, J. A. and Edgerton, V. R. (1999). Transmission of forces within mammalian skeletal muscles. *J. Biomech.* **32**, 371-380. doi:10.1016/S0021-9290(98)00189-4
Nishikawa, K. C., Monroy, J. A., Uyeno, T. E., Yeo, S. H., Pai, D. K. and Lindstedt, S. L. (2012). Is titin a "winding filament"? A new twist on muscle contraction. *Proc. Biol. Sci.* **279**, 981-990. doi:10.1098/rspb.2011.1304
Nocella, M., Colombini, B., Bagni, M. A., Bruton, J. and Cecchi, G. (2012). Non-crossbridge calcium-dependent stiffness in slow and fast skeletal fibres from mouse muscle. *J. Muscle Res. Cell Motil.* **32**, 403-409. doi:10.1007/s10974-011-9274-5
Ottenheijm, C. A. C., Voermans, N. C., Hudson, B. D., Irving, T., Stienen, G. J. M., van Engelen, B. G. and Granzier, H. (2012). Titin-based stiffening of muscle fibers in Ehlers-Danlos Syndrome. *J. Appl. Physiol.* **112**, 1157-1165. doi:10.1152/japplphysiol.01166.2011
Patel, T. J. and Lieber, R. L. (1997). Force transmission in skeletal muscle: from actomyosin to external tendons. *Exerc. Sport Sci. Rev.* **25**, 321-363. doi:10.1249/00003677-199700250-00014
Pollack, G. H. (1990). *Muscles & Molecules: Uncovering the Principles of Biological Motion*. Seattle, WA: Ebner & Sons Publishers.
Powers, K., Schappacher-Tilp, G., Jinha, A., Leonard, T., Nishikawa, K. and Herzog, W. (2014). Titin force is enhanced in actively stretched skeletal muscle. *J. Exp. Biol.* **217**, 3629-3636. doi:10.1242/jeb.105361

Powers, K., Nishikawa, K., Joumaa, V. and Herzog, W. (2016). Decreased force enhancement in skeletal muscle sarcomeres with a deletion in titin. *J. Exp. Biol.* **219**, 1311-1316. doi:10.1242/jeb.132027

Powers, K., Joumaa, V., Jinha, A., Moo, E. K., Smith, I. C., Nishikawa, K. and Herzog, W. (2017). Titin force enhancement following active stretch of skinned skeletal muscle fibres. *J. Exp. Biol.* **220**, 3110-3118. doi:10.1242/jeb.153502

Prado, L. G., Makarenko, I., Andresen, C., Krüger, M., Opitz, C. A. and Linke, W. A. (2005). Isoform diversity of giant proteins in relation to passive and active contractile properties of rabbit skeletal muscles. *J. Gen. Physiol.* **126**, 461-480. doi:10.1085/jgp.200509364

Prasartwuth, O., Allen, T. J., Butler, J. E., Gandevia, S. C. and Taylor, J. L. (2006). Length-dependent changes in voluntary activation, maximum voluntary torque and twitch responses after eccentric damage in humans. *J. Physiol.* **571**, 243-252. doi:10.1113/jphysiol.2005.101600

Rack, P. M. H. and Westbury, D. R. (1969). The effects of length and stimulus rate on tension in the isometric cat soleus muscle. *J. Physiol.* **204**, 443-460. doi:10.1113/jphysiol.1969.sp008923

Rassier, D. E., MacIntosh, B. R. and Herzog, W. (1999). Length dependence of active force production in skeletal muscle. *J. Appl. Physiol.* **86**, 1445-1457. doi:10.1152/jappl.1999.86.5.1445

Reconditi, M., Brunello, E., Fusi, L., Linari, M., Martinez, M. F., Lombardi, V., Irving, M. and Piazzesi, G. (2014). Sarcomere-length dependence of myosin filament structure in skeletal muscle fibres of the frog. *J. Physiol.* **592**, 1119-1137. doi:10.1113/jphysiol.2013.267849

Reddish, F. N., Miller, C. L., Gorkhali, R. and Yang, J. J. (2017). Calcium dynamics mediated by the endoplasmic/sarcoplasmic reticulum and related diseases. *Int. J. Mol. Sci.* **18**, E1024. doi:10.3390/ijms18051024

Sacks, R. D. and Roy, R. R. (1982). Architecture of the hind limb muscles of cats: functional significance. *J. Morphol.* **173**, 185-195. doi:10.1002/jmor.1051730206

Saladin, K. S., Gan, C. A. and Cushman, H. N. (2017). *Anatomy & Physiology: the Unity of Form and Function*, 8th edn. New York, NY: McGraw-Hill Education.

Schiaffino, S. and Reggiani, C. (1994). Myosin isoforms in mammalian skeletal muscle. *J. Appl. Physiol.* **77**, 493-501. doi:10.1152/jappl.1994.77.2.493

Seow, C. Y. (2013). Hill's equation of muscle performance and its hidden insight on molecular mechanisms. *J. Gen. Physiol.* **142**, 561-573. doi:10.1085/jgp.201311107

Stephenson, D. G. and Wendt, I. R. (1984). Length dependence of changes in sarcoplasmic calcium concentration and myofibrillar calcium sensitivity in striated muscle fibres. *J. Muscle Res. Cell Motil.* **5**, 243-272. doi:10.1007/BF00713107

Street, S., Sheridan, M. and Ramsey, R. (1966). Some effects of extreme shortening on frog skeletal muscle. *MVC Quarterly* **2**, 90-99.

Terui, T., Sodnomtseren, M., Matsuba, D., Udaka, J., Ishiwata, S., Ohtsuki, I., Kurihara, S. and Fukuda, N. (2008). Troponin and titin coordinately regulate length-dependent activation in skinned porcine ventricular muscle. *J. Gen. Physiol.* **131**, 275-283. doi:10.1085/jgp.200709895

Terui, T., Shimamoto, Y., Yamane, M., Kobirumaki, F., Ohtsuki, I., Ishiwata, S., Kurihara, S. and Fukuda, N. (2010). Regulatory mechanism of length-dependent activation in skinned porcine ventricular muscle: role of thin filament cooperative activation in the Frank-Starling relation. *J. Gen. Physiol.* **136**, 469-482. doi:10.1085/jgp.201010502

Trombitás, K., Greaser, M., French, G. and Granzier, H. (1998). PEVK extension of human soleus muscle titin revealed by immunolabeling with the anti-titin antibody 9D10. *J. Struct. Biol.* **122**, 188-196. doi:10.1006/jsbi.1998.3984

Walker, J. S., Li, X. and Buttrick, P. M. (2010). Analysing force–pCa curves. *J. Muscle Res. Cell Motil.* **31**, 59-69. doi:10.1007/s10974-010-9208-7

Wang, K., McClure, J. and Tu, A. (1979). Titin: major myofibrillar components of striated muscle. *Proc. Natl. Acad. Sci. USA* **76**, 3698-3702. doi:10.1073/pnas.76.8.3698

Witt, C. C., Ono, Y., Puschmann, E., McNabb, M., Wu, Y., Gotthardt, M., Witt, S. H., Haak, M., Labeit, D., Gregorio, C. C. et al. (2004). Induction and myofibrillar targeting of CARP, and suppression of the Nkx2.5 pathway in the MDM mouse with impaired titin-based signaling. *J. Mol. Biol.* **336**, 145-154. doi:10.1016/j.jmb.2003.12.021